

Crystallization and characterization of $\text{Pb}_2\text{Nb}_2\text{O}_7$ thin films prepared at high pressure and low temperature

Chung-Han Wu, Mohammad Qureshi, Chung-Hsin Lu*

Department of Chemical Engineering, Electronic and Electro-optical Ceramics Laboratory, National Taiwan University, Taipei, Taiwan, ROC

Abstract

A facile thin film crystallization of pyrochlore $\text{Pb}_2\text{Nb}_2\text{O}_7$ at low temperatures has been demonstrated at high pressures over rapid thermal annealing process (RTA). The crystallization of $\text{Pb}_2\text{Nb}_2\text{O}_7$ has started at temperatures as low as 220 °C. Powder X-ray diffraction patterns reveal the formation of pyrochlore phase without any intermediate phase formation. Scanning electron microscopy (SEM) and atomic force microscopy (AFM) features show the temperature dependence of crystal growth in both high pressure and RTA methods. Using the high-pressure method, the crystallization temperatures of $\text{Pb}_2\text{Nb}_2\text{O}_7$ are reduced to 220 °C when compared to 600 °C required for crystallization using RTA process. The uniform and dense structure that consisted of small grains with the size of 20–30 nm existed in the $\text{Pb}_2\text{Nb}_2\text{O}_7$ thin films heated by RTA process, whereas the use of high pressure modified the crystallize size to approximately 40–45 nm with island structures observed throughout the $\text{Pb}_2\text{Nb}_2\text{O}_7$ films.

© 2007 Elsevier Ltd. All rights reserved.

Keywords: A. Thin films; B. Chemical synthesis; D. Microstructure

1. Introduction

Electro-ceramic thin films have attracted considerable interest for applications in non-volatile ferroelectric random access memories due to their large reversible spontaneous polarization [1,2] and high dielectric permittivity [3–7]. In particular, compounds with the pyrochlore structure possess the distinctive characters such as: the low synthetic temperature, the facility for processing, the good chemical stability, the paraelectric property, the relative high dielectric constant, and interesting optical properties [8,9]. Therefore, the pyrochlore compounds become promising materials for the use in charge storage capacitors or in the application of memory thin films. $\text{Pb}_2\text{Nb}_2\text{O}_7$ ceramic is one of such paraelectric materials in room temperature having pyrochlore structure which has a dielectric constant of 190. $\text{Pb}_2\text{Nb}_2\text{O}_7$ has octahedral NbO_6 in the tetragonal structure with encircled Pb_2O in annular conformation. This material has attracted great attention for its low-temperature formation while synthesizing ferroelectric $\text{Pb}(\text{Zr},\text{Ti})\text{O}_3$ – $\text{Pb}(\text{Ni}_{1/3}\text{Nb}_{2/3})\text{O}_3$ ceramics

or other oxides of lead and niobium. In spite of having technological importance of $\text{Pb}_2\text{Nb}_2\text{O}_7$, there are very few literature reports available on the synthesis and characterization of this pyrochlore [10,11]. In our early efforts, we have demonstrated the synthesis of nanosize $\text{Pb}_2\text{Nb}_2\text{O}_7$ ceramic powder and other ceramic thin films by hydrothermal process [12,13], where in the single phase, $\text{Pb}_2\text{Nb}_2\text{O}_7$ powder was obtained at considerably low temperature such as 150 °C. The low crystallizing temperature and high dielectric constant makes the $\text{Pb}_2\text{Nb}_2\text{O}_7$ compound as the potential candidate for the application to thin film capacitors. In this paper we present a facile low temperature, high-pressure route for the crystallization of $\text{Pb}_2\text{Nb}_2\text{O}_7$ thin films fabricated by metal–organic decomposition (MOD) method.

2. Experimental

In the present study, $\text{Pb}_2\text{Nb}_2\text{O}_7$ thin films were fabricated by MOD method. The starting materials lead 2-ethylhexanoate [$\text{Pb}(\text{C}_8\text{H}_{15}\text{O}_2)_2$], niobium ethoxide [$\text{Nb}(\text{OC}_2\text{H}_5)_4$], with toluene as solvent mixed in stoichiometric ratio in a glove box to prepare the precursors needed

*Corresponding author. Tel.: +886 2 2365 1428; fax: +886 2 2362 3040.
E-mail address: chlu@ntu.edu.tw (C.-H. Lu).

for MOD method. The substrates were of the structure Pt/Ti/SiO₂/Si. Pt layer acts as the bottom electrode while Ti layer is used to enhance the adhesion of Pt layer to the silicon substrate. The Pt bottom electrode exhibited (1 1 1) plane preferred orientation. Before coating, the substrates were cut into small chip of dimension of 1 cm × 1 cm and then cleaned by RCA wet cleaning methods. The prepared precursor was spin-coated onto the cleaned substrates. Thin films were baked on the hot plate at 150 °C after coating in order to remove the excess of toluene solvent. Subsequently, the film with organic raw materials was pyrolyzed at 350 °C to form the amorphous phase. The spinning–baking–pyrolyzing cycle was repeated several times to obtain the proper film thickness. Thereafter, the amorphous films were annealed at the temperature range of 500–650 °C in flowing oxygen with different heating rates and soaking times.

In the designed process of altering crystallization, a high-pressure apparatus with an elaborate temperature controller was employed so as to change the process pressure with the temperature. A sealed stainless-steel (T316-SS) bomb was used as the autoclave container. The bottom of the bomb was filled with distilled water to produce a high vapor-pressure environment at elevated temperatures. The crystallization temperature of this developed process was adopted in the range of 220–300 °C with the heating rate of 10 °C/min. The composing phases of the synthesized films were characterized by X-ray diffraction (XRD) at room temperature using a MAC Science MXP3 XRD system with Cu K_α radiation at 40 kV and 30 mA. The surface morphologies were analyzed by scanning electron microscopy (SEM) (Hitachi model S-800 microscope, 20 kV) and atomic force microscopy (AFM) using tapping mode with amplitude modulation (Nanoscope IIIa, Digital Instruments Company, Santababara).

3. Results and discussion

3.1. Crystallization of Pb₂Nb₂O₇ thin films annealed by rapid thermal annealing (RTA) process

The solution of prepared precursors was spin-coated onto the Pt/Ti/SiO₂/Si substrates and then baked at 150 °C to remove the solvent. In order to burn out the organic species, the as-coated thin films were subsequently pyrolyzed at 350 °C for 30 min. By XRD analysis, there was no crystal structure found on the as-deposited thin films and the post-annealing was required for crystallizing Pb₂Nb₂O₇ thin films. Fig. 1 shows the XRD patterns of Pb₂Nb₂O₇ thin films annealed at various temperatures for 10 min using RTA equipment. From Fig. 1, it is evident that crystallized structure started to form at the temperature higher than 500 °C while the crystallization obtained was proved to be the phase of pyrochlore Pb₂Nb₂O₇ by the comparison of JCPDS file no. 40-828. As the annealing temperature increased to 600 °C, the crystallization of Pb₂Nb₂O₇ thin films was enhanced and only the diffraction peaks of Pb₂Nb₂O₇ were detected. However, no apparent

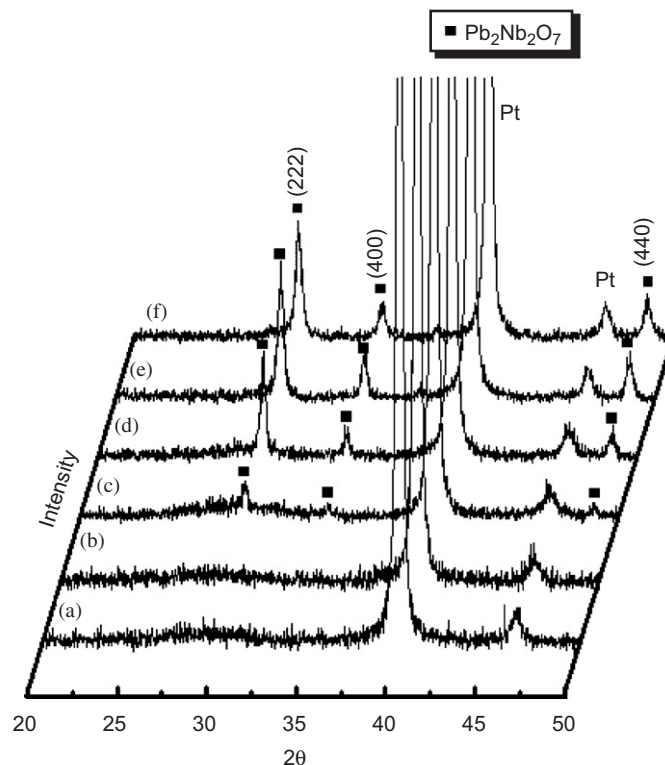


Fig. 1. Powder X-ray diffraction patterns of Pb₂Nb₂O₇ thin films annealed by rapid thermal annealing at varied temperatures: (a) as-pyrolyzed, (b) 450 °C, (c) 500 °C, (d) 550 °C, (e) 600 °C, (f) 650 °C.

improvement for the crystallization of Pb₂Nb₂O₇ thin film was observed as the annealing temperature rose to 650 °C. From the above results, the Pb₂Nb₂O₇ thin films were completely crystallized at the annealing temperature of 600 °C. There was no intermediate phase generated at the temperature below 500 °C, indicating the formation of crystallized Pb₂Nb₂O₇ thin films was nucleated directly from the amorphous precursor phase. The main diffraction peaks of these films were (2 2 2), (4 0 0), and (4 4 0). By comparing the intensity of diffraction peaks with those in JCPDS file, there was no special orientation existing in the crystallized Pb₂Nb₂O₇ thin films.

The SEM features of Pb₂Nb₂O₇ thin films annealed at various temperatures are shown in Fig. 2(a). The microstructure of amorphous thin films annealed at 450 °C was dense and flat and gradual increase in the grain growth was observed with increase in temperature up to 600 °C. Fig. 2(a) shows the SEM features when the annealing temperature rose to 600 °C, showing a uniform and dense film feature consisting of well-developed small grains, and no apparent difference of microstructure was made by the subsequent increase of annealing temperature to 650 °C on the thin film with the morphology of small sphere (around 20–30 nm). Inset in Fig. 2(a) shows the representative SEM features of a 550 °C annealed sample which shows the initial stage of Pb₂Nb₂O₇ film crystallization.

The surface morphology and film roughness of Pb₂Nb₂O₇ thin films heated by RTA process was observed by AFM. Fig. 2(b) shows the representative AFM image of

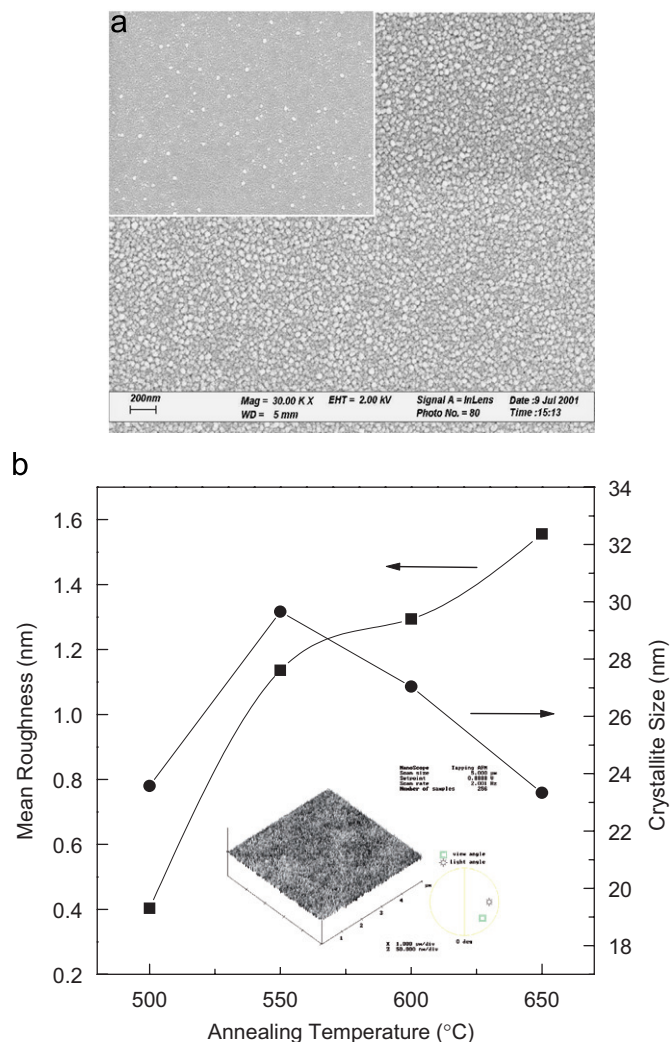


Fig. 2. (a) Scanning electron microscope images of $\text{Pb}_2\text{Nb}_2\text{O}_7$ on Pt/Ti/SiO₂/Si substrate annealed by rapid thermal annealing at 600 °C. Inset shows the representative SEM feature of $\text{Pb}_2\text{Nb}_2\text{O}_7$ by RTA process at 550 °C. (b) Temperature dependence of crystallite size and roughness as $\text{Pb}_2\text{Nb}_2\text{O}_7$ thin films annealed by RTA process. Inset shows the atomic force microscope image of $\text{Pb}_2\text{Nb}_2\text{O}_7$ thin films crystallized by RTA process at 600 °C.

$\text{Pb}_2\text{Nb}_2\text{O}_7$ thin film annealed at 600 °C. The $\text{Pb}_2\text{Nb}_2\text{O}_7$ thin films annealed at the rising temperatures above 600 °C had no variation in the surface morphology. In contrast with the results of high-pressure process, the surface morphology of $\text{Pb}_2\text{Nb}_2\text{O}_7$ thin films crystallized by RTA process depended less on the heating temperature. The similar subject on the relation between the crystallite size and the roughness of the thin films crystallizing by RTA process is also discussed. The crystallite size was calculated by the Debye–Scherrer formula. As observed by AFM, the roughness of $\text{Pb}_2\text{Nb}_2\text{O}_7$ thin films increased from 0.40 to 1.56 nm as the annealing temperature rose from 500 to 650 °C. The crystallite size of $\text{Pb}_2\text{Nb}_2\text{O}_7$ thin films annealed at 500 °C was about 23.6 nm, and the small crystallite was attributed to the low heating temperature. However, the variation in crystallite size with the increase in annealing

temperature was opposite from the variation in roughness while the heating temperature rose above 550 °C. The phenomenon observed that the crystallite size decreased as the annealing temperature increased was due to the greater heating rate of RTA process. The heating rate of 30 °C/s induced the shortening of heating time from room temperature to the annealing temperature. By the transient heating progress, the assumption that no crystallite formed while process temperature increasing was reasonable.

The $\text{Pb}_2\text{Nb}_2\text{O}_7$ crystallite nucleated after reaching the annealing temperature and the rise of annealing temperature led to the increase of $\text{Pb}_2\text{Nb}_2\text{O}_7$ nuclei. Thus, the grain growth of $\text{Pb}_2\text{Nb}_2\text{O}_7$ was inhibited by the increase of nuclei, and the crystallite sizes of $\text{Pb}_2\text{Nb}_2\text{O}_7$ thin films were decreased with the increase of annealing temperature. The increase of roughness was not due to the increase of crystallite size but was ascribed to the increase of $\text{Pb}_2\text{Nb}_2\text{O}_7$ grains that were crystallized by RTA process with the steep rise of the heating rates. The shortcomings of using RTA process is the small crystallite size and high-crystallization temperature which we tried to overcome by using high-pressure process described in the later section.

3.2. Crystallization of $\text{Pb}_2\text{Nb}_2\text{O}_7$ thin films under high-pressure condition

The high-pressure process was adopted to decrease the crystallization temperature and to increase the crystallite size of $\text{Pb}_2\text{Nb}_2\text{O}_7$ thin films. The as-deposited thin films were placed in a high-pressure apparatus after being pyrolyzed at 350 °C for the removal of organic components. Fig. 3 displays the XRD patterns of $\text{Pb}_2\text{Nb}_2\text{O}_7$ thin films crystallized at various temperatures within the range of 220–300 °C by high-pressure process. As the thin films heated at 220 °C with the process pressure of 300 psi, crystallization started on the $\text{Pb}_2\text{Nb}_2\text{O}_7$ thin films. The obvious crystallization of $\text{Pb}_2\text{Nb}_2\text{O}_7$ thin films was obtained as the heating temperature and process pressure rises to 260 °C and 624 psi. According to the diffraction pattern of $\text{Pb}_2\text{Nb}_2\text{O}_7$ thin films heated at 280 °C and 624 psi, the crystallization of $\text{Pb}_2\text{Nb}_2\text{O}_7$ thin films was enhanced with the increase of heating temperature and process pressure. The $\text{Pb}_2\text{Nb}_2\text{O}_7$ thin films crystallized by high-pressure process remained single phase even when the heating temperature and process pressure rose to 300 °C and 1150 psi. Similar to the RTA process, it could be seen that no intermediate phase was observed as thin films heated at the temperature range of 220–260 °C that $\text{Pb}_2\text{Nb}_2\text{O}_7$ started to crystallize, the phenomenon indicated that the formation of crystallized $\text{Pb}_2\text{Nb}_2\text{O}_7$ thin films is nucleated directly from the amorphous phase. The main diffraction peaks of these thin films were (2 2 2), (4 0 0), and (4 4 0) without the occurrence of special orientation. The crystallinity of $\text{Pb}_2\text{Nb}_2\text{O}_7$ thin films by high-pressure process coincided well with that of the RTA samples, though the crystallization temperature was reduced from 600 to 280 °C.

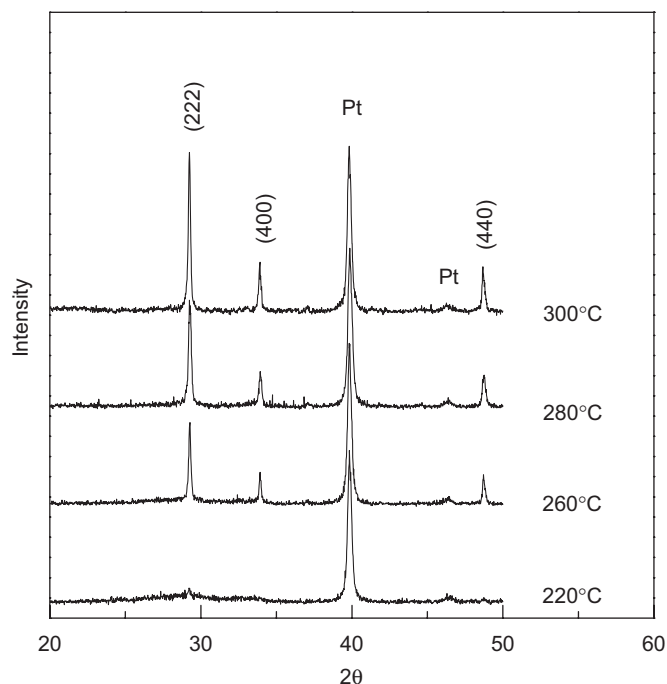


Fig. 3. Powder X-ray diffraction analysis for the $\text{Pb}_2\text{Nb}_2\text{O}_7$ thin films crystallized by high-pressure process at varied heating temperatures.

Fig. 4(a) shows the SEM micrographs of $\text{Pb}_2\text{Nb}_2\text{O}_7$ thin films crystallized by high-pressure process. The microstructure of amorphous thin films was flat without the observation of grains. As the $\text{Pb}_2\text{Nb}_2\text{O}_7$ thin films heated at 220°C with the process pressure of 300 psi, few special clusters of grains with an irregular shape were generated, the similar phenomenon was observed as crystallizing the Ta_2O_5 thin films by high-pressure process. As the heating temperature and process pressure increased to 260°C and 624 psi, the number of clusters was obviously increased. With the increase in temperature to 280°C at the process pressure of 864 psi, the surface of $\text{Pb}_2\text{Nb}_2\text{O}_7$ thin film was covered with the clusters of grains while the size of these clusters were around 100–200 nm. Special phenomenon that the cluster combined to form the larger one was observed as the heating temperature increased to 300°C with the process pressure of 1150 psi. From the results obtained by XRD and SEM analysis, the clusters of grains are supported to be the crystals of $\text{Pb}_2\text{Nb}_2\text{O}_7$, since the well-crystallized $\text{Pb}_2\text{Nb}_2\text{O}_7$ thin films possess the microstructure of grains in clusters.

Fig. 4(b) illustrates the relation between the crystallite size and the roughness of $\text{Pb}_2\text{Nb}_2\text{O}_7$ thin films as adopting high-pressure process for thin film crystallization. The roughness of the thin films was observed by AFM analysis while the crystallite size of $\text{Pb}_2\text{Nb}_2\text{O}_7$ was calculated from the width at the half maximum of the (222) peak by the Debye–Scherrer formula. As shown in Fig. 4(b), the crystallite size of $\text{Pb}_2\text{Nb}_2\text{O}_7$ increased with the increase of heating temperature. As the crystallization temperature rose from 220 to 300°C , the crystallite size increased from 46.0 to 48.9 nm though the difference of these crystallites size was merely around 6% in the temperature range of 80°C . Moreover, the roughness of

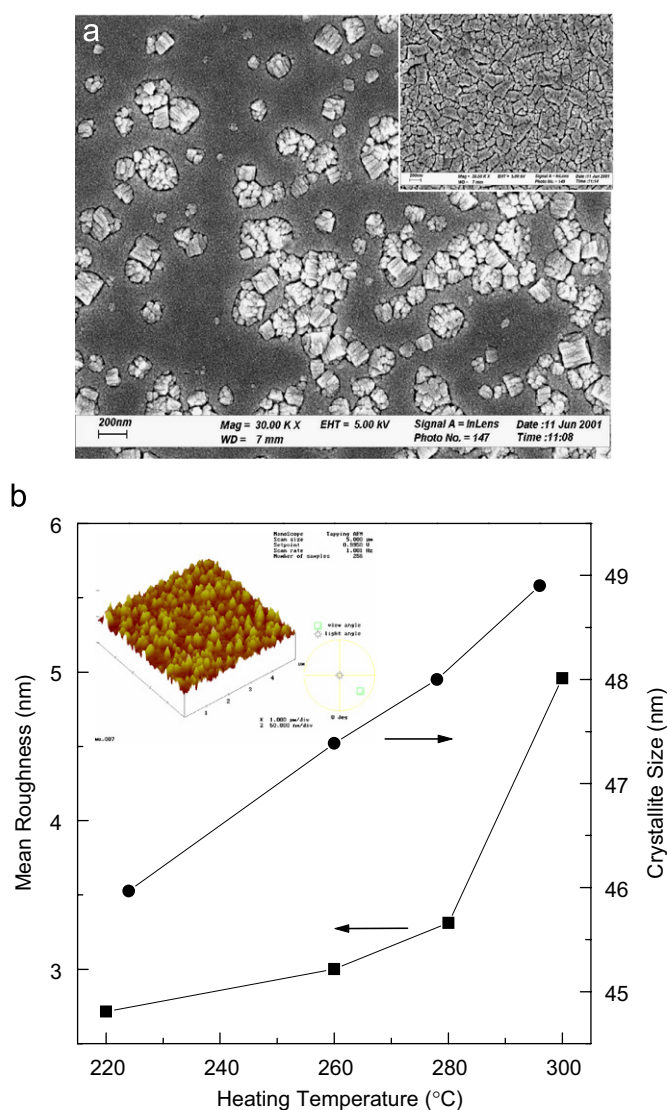


Fig. 4. (a) Scanning electron microscope images of $\text{Pb}_2\text{Nb}_2\text{O}_7$ thin films crystallized by high-pressure process at 260°C . Inset shows the microscopic features of the film processed at 300°C . (b) Temperature dependence of crystallite size and roughness as $\text{Pb}_2\text{Nb}_2\text{O}_7$ thin films crystallized by high-pressure process. Inset shows the atomic microscopic image of the sample processed at 300°C .

thin films was also increased with the increase in the temperature, the mean roughness increased from 2.72 to 4.96 nm. In comparison with the SEM results, the increase of roughness was ascribed to the increased number of grain clusters that formed on the thin films with the rising of heating temperature. Furthermore, there were similar tendencies for both crystallite size and roughness to increase as the crystallization temperature increased. The increment of roughness could also be partially attributed to the enlargement of crystallite size while adopting the high-pressure process for $\text{Pb}_2\text{Nb}_2\text{O}_7$ thin film crystallization. Inset in Fig. 4(b) shows the representative AFM image of surface morphology of $\text{Pb}_2\text{Nb}_2\text{O}_7$ thin films crystallized by high-pressure process at 300°C . The scan area is $5\ \mu\text{m} \times 5\ \mu\text{m}$. The $\text{Pb}_2\text{Nb}_2\text{O}_7$ crystallites formed on the surface of films

possessed the similar island structure that was also found as crystallizing the Ta₂O₅ thin films [14]. As the heating temperature and pressure increased to 260 °C and 624 psi, denser morphology was obtained with the increase of island number and crystallite size. The size of island structure was enhanced obviously with the increase of temperature and pressure. The rougher surface of Pb₂Nb₂O₇ thin films was generated when the heating temperature reached 300 °C with the process pressure of 1150 psi. The rougher morphology observed was attributed to the combination of cluster as contrast to the SEM micrograph.

4. Conclusions

We have demonstrated a facile low temperature, high-pressure crystallization process of pyrochlore Pb₂Nb₂O₇ comparing the well-known RTA with that of the high-pressure method. Powder X-ray patterns of Pb₂Nb₂O₇ synthesized by both the methods show initial crystallization temperatures of 500 and 200 °C by RTA and high-pressure methods, respectively. SEM and AFM features reveal that the high-pressure method is superior in forming special large crystals at low temperatures compared to the small dense crystallites using RTA method. With the increase in temperatures, the rate of increase in crystallinity is high in case of high-pressure method, whereas RTA method is not highly temperature sensitive after certain temperature range. By adopting the high-pressure process, the starting temperature for the crystallization was reduced from 600 to 220 °C.

References

- [1] C.A. De Araujo Paz, J.D. Cuchiaro, M.C. Scott, L.D. Mcmillan, Fatigue-free ferroelectric capacitors with platinum electrodes, *Nature* 374 (1995) 627–629.
- [2] Y. Tarui, T. Horai, K. Termoto, H. Koike, K. Nagashima, Application of the ferroelectric materials to ULSI memories, *Appl. Surf. Sci.* 114 (1997) 656–663.
- [3] K. Amanuma, T. Hase, Y. Miyasaka, Preparation and ferroelectric properties of SrBi₂Ta₂O₉ thin films, *Appl. Phys. Lett.* 66 (1995) 221–223.
- [4] P.Y. Chu, R.E. Jones Jr., P. Zurcher, D.J. Taylor, B. Jiang, S.L. Gillespie, Y.T. Lii, Characteristics of spin-on ferroelectric SrBi₂Ta₂O₉ thin film capacitors for FERAM application, *J. Mater. Res.* 11 (1996) 1065–1069.
- [5] H.M. Yang, J.S. Luo, W.T. Lin, In situ growth of fatigue free SrBi₂Ta₂O₉ films by pulsed laser ablation, *J. Mater. Res.* 12 (1997) 1145–1151.
- [6] C.H. Lu, B.K. Fang, Secondary phase formation and microstructural development in the interaction between SrBi₂Ta₂O₉ films and Pt/Si/SiO₂/Si substrates, *J. Mater. Res.* 12 (1997) 2104–2110.
- [7] A.I. Kingon, J.P. Maria, S.K. Streiffer, Alternative dielectrics to silicon dioxide for memory and logic devices, *Nature* 406 (2000) 1032–1038.
- [8] C.H. Lu, Y.C. Chen, Y.C. Sun, Low-temperature crystallization of electroceramic thin films at elevated pressure, *J. Mater. Chem.* 12 (2002) 1628–1630.
- [9] V. Natarajan, M.K. Bhide, A.R. Dhobale, S.V. Godbole, T.K. Seshagiri, A.G. Page, C.H. Lu, Photoluminescence, thermally stimulated luminescence and electron paramagnetic resonance of europium-ion doped strontium pyrophosphate, *Mater. Res. Bull.* 39 (2004) 2065–2075.
- [10] S.Y. Chen, C.M. Wang, S.Y. Cheng, The effect of pyrochlore phase on formation mechanism and electrical properties of perovskite PZMN relaxors, *Mater. Chem. Phys.* 49 (1995) 70–77.
- [11] O. Babushkin, T. Lindback, J.C. Luc, J.Y.M. Leblais, Reaction sequence in the formation of perovskite Pb(Zr_{0.48}Ti_{0.52})O₃–Pb(Nb_{2/3}Ni_{1/3})O₃ solid solution: dynamic heat-treatment, *J. Eur. Ceram. Soc.* 18 (1998) 737–744.
- [12] C.H. Lu, W.H. Wu, Photocatalytic TiO₂ thin films prepared via a high-pressure crystallization process, *Mater. Sci. Eng. B* 113 (2004) 42–45.
- [13] C.H. Lu, S.Y. Lo, Lead pyroniobate pyrochlore nanoparticles synthesized via hydrothermal processing, *Mater. Res. Bull.* 32 (1997) 371–378.
- [14] C.H. Lu, C.H. Wu, *J. Eur. Ceram. Soc.* 26 (2006) 2753.